JACS
JOURNAL OF THE AMERICAN CHEMICAL SOCIETY
Article
pubs.acs.org/JACS

Carbon Dioxide Capture by an Amine Functionalized Ionic Liquid: Fundamental Differences of Surface and Bulk Behavior

Inga Niedermaier,[†] Matthias Bahlmann,[‡] Christian Papp,*[,†] Claudia Kolbeck,[†] Wei Wei,[‡] Sandra Krick Calderón,[†] Mathias Grabau,[†] Peter S. Schulz,[‡] Peter Wasserscheid,[‡] Hans-Peter Steinrück,[†] and Florian Maier*[,†]

[†]Lehrstuhl für Physikalische Chemie II and [‡]Lehrstuhl für Chemische Reaktionstechnik, Universität Erlangen-Nürnberg, Egerlandstraße 3, 91058 Erlangen, Germany

Supporting Information

ABSTRACT: Carbon dioxide (CO_2) absorption by the amine-functionalized ionic liquid (IL) dihydroxyethyl dimethylammonium taurinate at 310 K was studied using surface- and bulk-sensitive experimental techniques. From near-ambient pressure X-ray photoelectron spectroscopy at 0.9 mbar CO_2, the amount of captured CO_2 per mole of IL in the near-surface region is quantified to ∼0.58 mol, with ∼0.15 mol in form of carbamate dianions and ∼0.43 mol in form of carbamic acid. From isothermal uptake experiments combined with infrared spectroscopy, CO_2 is found to be bound in the bulk as carbamate (with nominally 0.5 mol of CO_2 bound per 1 mol of IL) up to ∼2.5 bar CO_2, and as carbamic acid (with nominally 1 mol CO_2 bound per 1 mol IL) at higher pressures. We attribute the fact that at low pressures carbamic acid is the dominating species in the near-surface region, while only carbamate is formed in the bulk, to differences in solvation in the outermost IL layers as compared to the bulk situation.

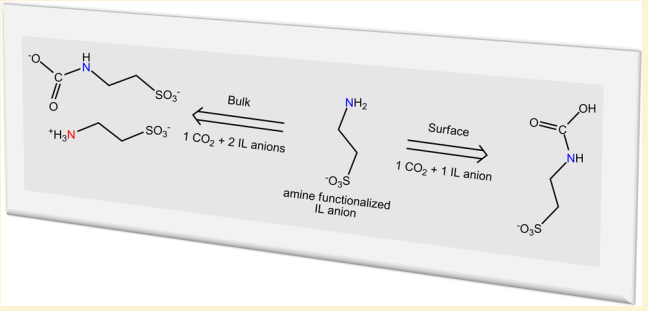

1. INTRODUCTION

Carbon dioxide (CO_2) emissions increased drastically since the start of the industrial age, leading to atmospheric CO_2 levels nowadays of more than 30% higher as compared to preindustrial times.[1] Atmospheric enrichment of this greenhouse gas most likely causes global warming. Therefore, possibilities to counteract this detrimental development are widely discussed. Removal of CO_2 from industrial flue gases is one of the main starting points toward lowering the annual CO_2 release. The most advanced and most promising technology is the scrubbing of flue gases with amines such as aqueous monoethanolamine (MEA) solutions,[2] which chemically and reversibly bind CO_2 by carbamate formation.[1,3] This amine scrubbing is already widely applied in natural gas sweetening and air recycling in confined spaces such as submarines[4,5] but until now not fully tested for postcombustion CO_2 capture in large-scale power plants.[1]

The use of MEA or other amine-based technologies has certain drawbacks. Specifically, the corrosiveness of the substances and their instability and volatility at elevated temperatures cause environmental, technical, and economic concerns.[1,3,6−8] In 1999, ionic liquids (ILs) were introduced as potential replacements for MEA in CO_2 absorption.[9] ILs are a class of compounds composed solely of ions with a melting point below 100 °C, or very often even below room temperature.[10] In comparison to MEA, ILs usually are thermally more stable and exhibit an extremely low vapor pressure.[1,3,7] Several studies have shown that simple, nonfunctionalized ILs are able to dissolve CO_2 quite well.[1,6,7] However, the physical absorption capacity of these ILs cannot compete with MEA.[1,6]

To increase CO_2 uptake capacity, the idea of functionalizing ILs with amine groups to bind CO_2 not only physically but also chemically was put forward by Bates et al.[11] They, and later Galán Sánchez et al., studied ILs containing an amine-functionalized imidazolium cation.[11,12] The CO_2 capture capability of several amino-acid-based ILs was examined by the Brennecke group,[13,14] and Soutullo et al. investigated a large set of ammonium ILs, containing a secondary amine as part of a sulfonate anion.[5] Recently, Schneider and co-workers outlined efficient CO_2 capture strategies, which are based on first-principles gas phase calculations.[15] With respect to ILs functionalized with primary amines, they particularly investigated the possible CO_2 capture steps 1−4 according to Scheme 1:

In analogy to aqueous alkanolamine systems such as MEA, the initial capture reaction of the Lewis acid CO_2 with the basic R-NH_2 group (R represents either a cationic or an anionic substituent of the IL) is given by reaction 1 of Scheme 1, forming carbamic acid (R−NH−COOH). Depending on the environment, the latter consecutively deprotonates (2), and the

Received: October 24, 2013
Published: December 9, 2013

dx.doi.org/10.1021/ja410745a | J. Am. Chem. Soc. 2014, 136, 436−441

Scheme 1. Reaction Scheme for Reacting an IL Functionalized with Primary Amines with CO_2 (R: cationic or anionic substituent)[15]

$$R\text{-}NH_2 + CO_2 \longrightarrow R\text{-}NHCOOH \quad (1)$$

$$R\text{-}NHCOOH \longrightarrow R\text{-}NHCOO^- + H^+ \quad (2)$$

$$R\text{-}NH_2 + H^+ \longrightarrow R\text{-}NH_3^+ \quad (3)$$

$$2\ R\text{-}NH_2 + CO_2 \longrightarrow R\text{-}NHCOO^- + R\text{-}NH_3^+ \quad (4)$$

proton is transferred (3) to another amine acting as base, to form a carbamate ($R-NH-COO^-$) and an ammonium ($R-NH_3^+$) species. The overall reaction 4 of primary amines with CO_2 to carbamate results in a nominal molar uptake of 1:2 = 0.5 (1 mol CO_2 per 2 mol amine).[1,6,15] If reaction (1) was the main reaction forming carbamic acid as the stable final product, the uptake capacity would be 1:1.

From their gas phase calculations for ion pairs, Schneider et al. predicted that, depending on the charge of the ionic substituent R, either the full reaction path (4) or only the initial reaction (1) is favored:[15] when the amine is bound to a cationic IL substituent R^+, deprotonation (2) is preferred, forming the zwitterion ($R^+-NH-COO^-$), which is stabilized by intramolecular Coulomb interactions. Note that the energetic costs of the concomitantly formed dication $R^+-NH_3^+$ in reaction 3 were not taken into account in these calculations. In contrast, when the amine group is bound to an anionic substituent R^-, carbamic acid is predicted to be stabilized, because of the electrostatically unfavored dianionic $R^--NH-COO^-$ carbamate formed in reaction 2. Here, the energetic gain by forming the consecutive $R^--NH_3^+$ zwitterion in reaction 3 was neglected. The authors noted that the above-described general tendency for either the 1:2 or the 1:1 mechanism might be a simplification because of the lack of screening effects in their gas phase calculations.[15] Indeed, Welton and co-workers showed that in the bulk of ILs very efficient charge screening occurs.[16] In collaboration with Schneider et al., the role of the ionic substituent carrying the amine group was investigated experimentally by the Brennecke group: in CO_2 uptake experiments employing ILs with amino acid anions, indeed a maximum 1:1 ratio of CO_2 to amine was found confirming the gas phase predictions.[13,14] In contrast, considerably lower maximum uptake ratios were found for ILs with amine-functionalized cations.[11]

The role of CO_2 fixation by carbamic acid is still under debate, which, among other difficulties, is related to ambiguities of NMR and IR signal assignments. Studies on ILs with amino-functionalized anions address different scenarios, (a) the simultaneous formation of carbamate and carbamic acid,[13] (b) the exclusive formation of carbamate as final product,[17] or (c) simply state the formation of carbamation products, without attempting to identify whether carbamate or carbamic acid is present.[5] This discussion about product species identity is not restricted to ILs. Publications on the reaction of CO_2 with amine-functionalized silica and titania surfaces also reveal contradictory interpretations of spectroscopic results by different authors.[18−20] Numerous studies identify substituent groups,[8,14] CO_2 partial pressure,[13] solvent properties,[21] proximity of charge centers in the case of charged substituents,[14] different possibilities of stabilization (e.g., by dimer formation or H-bonding),[18] or the presence of moisture[18,20] as potential factors that influence the carbamate−carbamic acid equilibrium. These ambiguities in experimental findings, particularly in supported systems with high surface area, demonstrate the need for additional experimental work to elucidate the important processes at the IL−gas interface, which are specifically relevant for the initial reaction steps.

To investigate the role of the IL-gas interface in the course of CO_2 fixation, we used X-ray photoelectron spectroscopy (XPS). In contrast to many other spectroscopic techniques, XPS provides a direct, quantitative, and element-specific access to the composition of the near-surface region of the studied solid or liquid materials, due to the small inelastic mean-free path of the excited photoelectrons (2−3 nm in ILs, depending on kinetic energy).[22] Taking advantage of the extremely low vapor pressure of ILs,[23] XPS thus has recently developed to an outstandingly powerful tool for IL surface and interface investigations under ultrahigh vacuum (UHV) conditions.[24] In this study, we employed a special near-ambient pressure (NAP) XPS chamber setup[25] to record for the first time XP spectra of ILs at CO_2 pressures up to 1 mbar; note that this pressure is the same order of magnitude as the atmospheric CO_2 partial pressure of ∼0.3 mbar.[26]

Scheme 2. CO_2 Reacting with the Amine-Functionalized IL $[Me_2N(CH_2CH_2OH)_2][H_2N(CH_2)_2SO_3]$ (center) to Form as Final Products Carbamic Acid or Carbamate in the 1:1 (right) or in the 1:2 (left) Mechanism, Respectively[a]

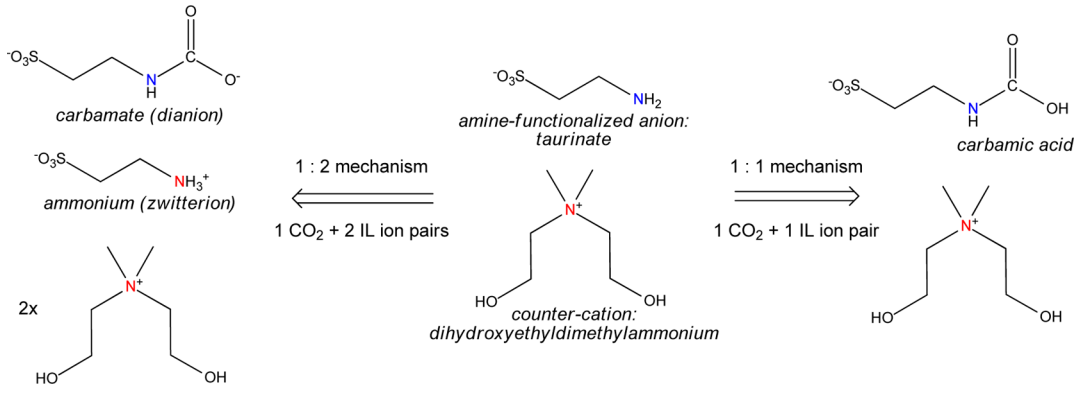

[a]All ammonium nitrogen atoms exhibiting a common XPS binding energy of about 403.0 eV are marked in red, whereas all neutral nitrogens at about 399.9 eV binding energy are shown in blue.

dx.doi.org/10.1021/ja410745a | J. Am. Chem. Soc. 2014, 136, 436−441

2. RESULTS AND DISCUSSION

As model system, we investigated the IL dihydroxyethyldimethylammonium taurinate ($[Me_2N(CH_2CH_2OH)_2][H_2N(CH_2)_2SO_3]$) (see Scheme 2, center). This IL carries the amine functional group as part of the sulfonate anion, whereas the ammonium cation is hydroxy-functionalized in analogy to MEA. Scheme 2 also shows the possible product molecules discussed in this study after reaction with CO_2. It is important to note that all species with a neutral nitrogen atom, i.e., amine, carbamate and carbamic acid, exhibit a very similar N 1s binding energy (atoms marked blue in Scheme 2) and are thus not discernible in XPS due to our limited energy resolution. In contrast, the signals of the positively charged ammonium nitrogen atoms of the IL cations and of the ammonium zwitterion (marked red in Scheme 2) are both shifted by about 3 eV toward higher binding energy. The very small N 1s chemical shifts between amine, carbamic acid and carbamate species, and the large shift for ammonium atoms were recently confirmed in a high-resolution XPS study of Lewis and coworkers applying synchrotron radiation to a liquid jet of an aqueous MEA solution.[27]

Prior to the NAP-XPS investigations, the IL was heated to 390 K for 1 h within the UHV chamber, to remove any airborne contaminations such as water or already reacted CO_2, and to obtain the pure IL at a defined initial state. Gas phase analysis by mass spectrometry during this heat treatment (not shown) revealed desorption of H_2O and CO_2 from the sample. The resulting N 1s and O 1s spectra of the degassed IL are shown in black in Figure 1. In the N 1s region, two peaks of

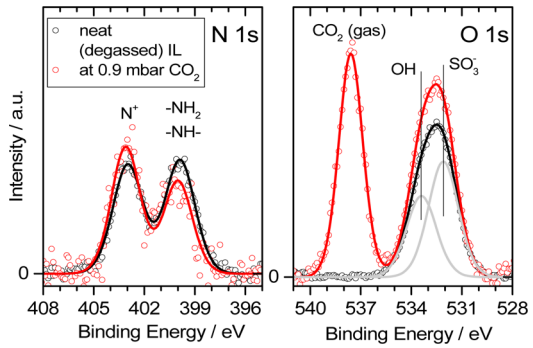

Figure 1. N 1s and O 1s spectra of the neat IL after degassing (black) and during CO_2 dosage at a background pressure of 0.9 mbar (red). The intensity of the spectra taken during CO_2 dosage are scaled to account for signal damping by the gas phase (see Experimental Section).

equal height are observed, which belong to the ammonium species in the cation (403.0 eV) and to the amine group in the anion (399.9 eV). The asymmetric signal in the O 1s spectrum also contains contributions of two different species: the two OH groups (533.4 eV) in the cation, and the three oxygen atoms of the sulfonate group in the anion (532.1 eV). The quantitative analysis of the N 1s, O 1s, S 2p, and C 1s core levels (the latter two can be found in the Supporting Information, Figure S1) confirms the nominal stoichiometry of the IL within ±5% uncertainty, which excludes major contamination (e.g., remaining CO_2).

After the degassing procedure, CO_2 was applied at a background pressure of 0.9 mbar at 310 K, while recording XP spectra. The corresponding N 1s and O 1s data are shown in red in Figure 1; note that the intensities are corrected for the overall signal attenuation due to scattering (damping) of the emitted photoelectrons by the CO_2 gas phase (see Experimental Section). Within the first minutes, the ammonium peak in the N 1s spectrum at 403.0 eV rapidly increased by +15% (±1%) of the original ammonium intensity, whereas the amine peak simultaneously decreased by the same amount, that is, −15% (±1%). The formation of additional ammonium is attributed to reaction pathway 4 in Scheme 1, that is, the 1:2 mechanism in Scheme 2 (left part): two taurinate anions react with one CO_2 molecule to the carbamate dianion (which does not affect the N 1s signal intensities) and the ammonium zwitterion, which leads to the observed intensity changes. Thus, from the N 1s spectra at 0.9 mbar CO_2 pressure, we have a clear indication that in the near-surface region probed by XPS, that is, within the XPS probing depth of ∼7−9 nm, ∼0.15 mol CO_2 are bound to ∼0.30 mol of the amine-functionalized IL anions via the carbamate/ammonium pathway, irrespective of the fact that this pathway might not be favored according to the predictions of Schneider et al.[15]

Along with the intensity changes in the N 1s region during CO_2 exposure, the IL-derived O 1s signals next to the CO_2 gas phase signal at 537.6 eV (see Figure 1) increase by +23% (±3%); this increase originates from the O 1s contributions of the formed COO-groups in the near-surface region (i.e., absorbed CO_2) that fall in the same binding energy range as the OH and SO_3^-. Note that, in contrast to the two N 1s signals, which are intrinsically referenced to each other, the uncertainty in the O 1s intensity changes is slightly increased, due the correction for the gas phase attenuation effect. Because one carbon dioxide molecule and one original IL ion pair contain two and five oxygen atoms, respectively, the observed oxygen increase of about 23 ± 3% directly translates in an average uptake ratio of ∼0.23 × 5/2 = ∼0.58 ± 0.08 mol CO_2 per ion pair within the XPS probing depth; this calculation is performed under the reasonable assumption that the molecular density does not change considerably during the adsorption process. The total uptake of ∼0.58 mol CO_2 notably exceeds the amount of ∼0.15 mol carbamate as witnessed by N 1s spectra. Because we can rule out significant amounts of physisorbed CO_2 (under our low pressure conditions) and also other sources for additional oxygen (such as water contamination; see Experimental Section), our XPS results clearly indicate that the additional CO_2 content is chemically bound in form of carbamic acid. Note that CO_2 adsorption was also confirmed by an intensity increase in the C 1s region, but quantification was less unambiguous compared to the oxygen increase due to the abundance of carbon atoms in the IL.

From the quantitative analysis of the N 1s and O 1s, we can derive the mean composition of the near-surface region, that is, within the XPS probing depth of ∼7−9 nm: Under a CO_2 pressure of 0.9 mbar, 1 mol of the taurinate anion is transformed into ∼0.15 mol carbamate as dianion, ∼0.15 mol ammonium as zwitterion, and ∼0.58 − 0.15 = ∼0.43 mol carbamic acid; the residual ∼0.27 mol taurinate remains unchanged.

Prolonged CO_2 exposure at 0.9 mbar at 310 K, even for two hours, did not lead to further changes in XP spectra demonstrating that a quasi-equilibrium situation in the near-surface region is reached within minutes. After switching off the CO_2 supply the pressure quickly dropped to $\sim 10^{-7}$ mbar within minutes, as expected from the pumping speed of the chamber. Thereafter, it decreased to its initial value of 10^{-9} mbar at a

dx.doi.org/10.1021/ja410745a | J. Am. Chem. Soc. 2014, 136, 436−441

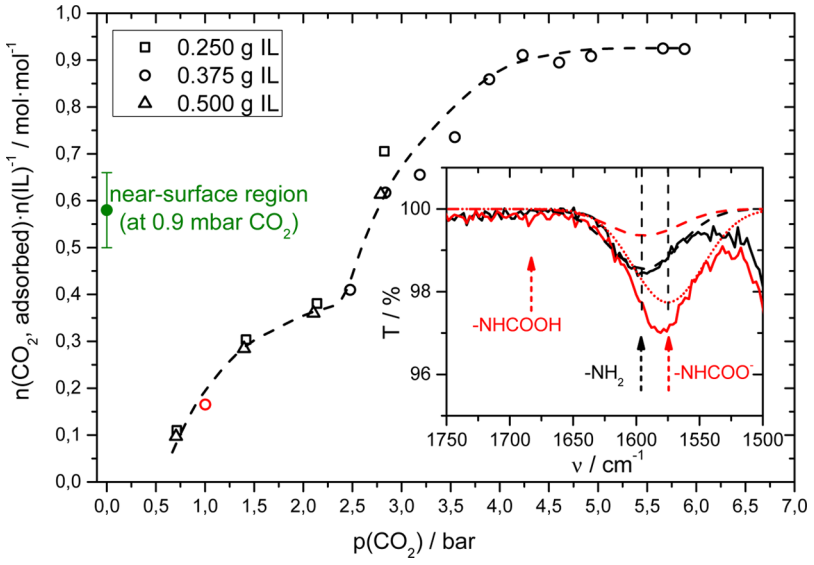

Figure 2. Bulk isothermal absorption curve at 310 K for CO_2 by $[Me_2N(CH_2CH_2OH)_2][H_2N(CH_2)_2SO_3]$; different amounts of IL are used to check for reproducibility and for transport limitation effects. Dashed line is to guide the eye. Inset: IR transmission spectra of the degassed IL (black) and after equilibrium absorption at 1 bar CO_2 (red) in the range of NH-bending modes and C═O stretching modes; indicated modes are discussed in the text.

slower rate. The characteristic time for this decrease scaled with the total CO_2 exposition time. On the same time scale of the slow pressure decrease, the XP spectra also recovered toward the original situation prior to CO_2 exposure, that is, comparable intensities of the two N 1s peaks (see Supporting Information Figure S3). Interestingly, the initial XP spectra of the nondegassed taurinate IL (i.e., the IL exposed for days to atmosphere with its natural CO_2 content of ∼0.3%) and also XP spectra of the IL after ex situ purging with 1 bar CO_2 (see next section) look virtually identical to the red spectra in Figure 1 (the corresponding N 1s spectra are shown in the Supporting Information, Figure S4). For these samples, storage in vacuum for several hours at room temperature did not lead to significant spectral changes; however, an enhanced background CO_2 pressure indicated a continuous outgassing of these CO_2-loaded ILs, particularly for the purged IL. Only after degassing at elevated temperatures in UHV, the black spectra of the neat IL shown in Figure 1 were recorded. These findings indicate that, upon CO_2 exposure, in the near-surface region, which is monitored during NAP XPS, quickly a quasi-equilibrium situation is reached, with a composition of ∼0.15 mol carbamate and ∼0.43 mol carbarmic acid. We propose that, from the near-surface region, slow diffusion of CO_2-loaded molecules occurs to the bulk, which serves as reservoir. After removal of the CO_2 gas phase, the diffusion process is reversed on a similar time scale. In this scenario, for the nondegassed sample and for the purged sample, with more CO_2 stored in the bulk, loss of CO_2 from the near-surface region by desorption into vacuum is compensated by diffusion of CO_2-loaded molecules from the bulk to the near-surface region to maintain the favorable surface situation. This also explains the much longer degassing time (or the required elevated degassing temperature) of these sample as compared to those prepared by exposure to CO_2 in the XPS chamber. Only after significant CO_2 depletion of the IL bulk, also the composition in the near-surface region changes and the XP spectra of the degassed neat IL are obtained.

To obtain a better understanding of the CO_2 capture process, we also investigated the CO_2 absorption process in the bulk of the same IL under equilibrium conditions by external absorption isotherms and infrared (IR) spectroscopy experiments (see Experimental Section for details). Figure 2 shows the amount of bound CO_2 per mol neat IL (i.e., per mol of amine groups) at 310 K as a function of equilibrium CO_2 pressure, from 0.5 up to 6.0 bar. Independent of the initial amount of degassed IL used (0.250, 0.375, or 0.500 g), the uptake curve exhibits a characteristic two-step behavior: around 2.5 bar, the uptake approaches a first step with about 0.4 mol CO_2 bound per mol IL. Above 2.5 bar, a second adsorption channel sets in, reaching a maximum uptake of about 0.92 mol CO_2 per mol IL at ∼4 bar. These characteristics fit well to the assumption that in the low pressure regime, CO_2 fixation in the bulk mainly occurs via carbamate formation via the 1:2 mechanism (overall reaction 4 in Scheme 1), and only for high pressures CO_2 fixation by carbamic acid in the 1:1 mechanism (reaction 1 in Scheme 1) becomes more favorable.

To confirm the hypothesis of carbamate as dominating bulk species at pressures below 2.5 bar, we also performed attenuated total reflectance infrared (ATR-IR) absorption measurements of the degassed IL immediately after the isothermal absorption experiment at 1 bar CO_2 (red circle in Figure 2). In the inset of Figure 2, the corresponding transmission IR spectra are shown in the region of interest for N−H bending and C−O stretching modes, as black and red solid curves, respectively. After CO_2 absorption, significant changes are observed: the peak of the neat IL (dashed black fit curve) at around 1594 cm^{-1}, assigned to the $-NH_2$ bending mode of the primary amine,[21] decreases in intensity (dashed red fit curve), and a new peak at around 1575 cm^{-1} appears (dotted red fit curve), which is assigned to the CO stretching mode of $-NCOO^-$ of carbamate.[21] Moreover, no absorption is visible in the region between 1650 and 1750 cm^{-1}, where the corresponding CO stretching mode of −NCOOH of carbamic acid should arise.[21,28]

dx.doi.org/10.1021/ja410745a | J. Am. Chem. Soc. 2014, 136, 436−441

In addition to IR, we also confirmed the presence of only one bulk species by the observation of only one single peak at 161.2 ppm in the ^{13}C NMR (see Supporting Information, Figure S2), which arises after purging the sample for 3 h with CO_2 at 1 bar. As noted in the beginning, a differentiation between carbamate and carbamic acid from absolute NMR signal positions is not unambiguously possible. However, in combination with IR, we can clearly assign the signal to the carbamate species alone.

The most striking message from Figure 2 is that at low pressures much more CO_2 is stored in the near-surface region than in the bulk (under equilibrium conditions and at the same temperature of 310 K): whereas the in situ XPS experiment shows that already at 0.9 mbar pressure ~0.58 mol CO_2 per mol IL are absorbed in the near-surface region (green data point in Figure 2) in a quasi-equilibrium situation, around 3 bar is required to obtain a similar value in the bulk. Moreover, in the near-surface region, carbamic acid is the dominating CO_2 carrier, whereas in the bulk at pressures at least up to 1 bar exclusively carbamate is present, as shown by IR. The difference in the nature of the CO_2 carrier in the near-surface region and in the bulk is attributed to a different degree of charge screening by solvation of the singly charged carbamic acid (right side of Scheme 2), and the doubly charged carbamate and ammonium (left side) species. It is known from angle-resolved XPS that neutral moieties are preferentially localized at the surface, whereas highly charged moieties have a strong tendency toward the bulk.[29] Along these lines, we thus propose that the carbamate dianion and the ammonium zwitterion are less favored in the near-surface region due to the lack of full solvation shells, but they are energetically stabilized in the bulk. Notably, for aqueous MEA solutions purged with CO_2, Lewis et al. also found surface enrichment of carbamic acid, whereas the bulk solution preferentially contained carbamate and ammonium.[27]

3. CONCLUSIONS

We have investigated the potential of the amine-functionalized IL dihydroxyethyldimethylammonium taurinate for CO_2 capture by a combination of surface- and bulk-sensitive experimental techniques. From near-ambient pressure XPS, we deduced that, at 310 K and a CO_2 pressure of 0.9 mbar, the near-surface composition is in a quasi-equilibrium situation with 1.00 mol of the taurinate anion transformed into ~0.15 mol carbamate as dianion and ~0.15 mol ammonium as zwitterion, ~0.43 mol carbamic acid, and the residual ~0.27 mol taurinate remaining unchanged. By a combination of isothermal uptake experiments under equilibrium conditions up to 6 bar CO_2 and infrared spectroscopy, CO_2 absorption in the bulk of this IL was found to occur stepwise: in a first step, the amount of captured CO_2 increases to ~0.4 mol per mol IL at 2.5 bar, indicative of carbamate formation, with a nominal storage capacity of 0.5 mol CO_2; in a second step, a value of ~0.92 mol CO_2 per mol IL is reached above 4 bar, indicative of reaction to carbamic acid, with a nominal storage capacity of 1.0 mol CO_2. The exchange of CO_2 between gas phase and near-surface region is proposed to be considerably faster than the transport of CO_2-carrying molecules between near-surface region and bulk. The fact that at low pressures carbamic acid is the dominating species in the near-surface region, while only carbamate and ammonium are formed in the bulk up to 2.5 bar, is attributed to an improved charge screening by solvation, which drives the doubly charged carbamate dianion and the ammonium zwitteranion into the bulk. Considering the XPS probing depth of 7−9 nm, which corresponds roughly to 10 layers of IL ion pairs, the observed concentration of carbamic acid could be understood by assuming a more or less complete conversion of taurinate to carbamic acid in the outermost molecular layer(s). This situation is quickly reached due to adsorption from the gas phase. Further absorption only occurs by conversion to carbamate as CO_2-carrying species, which then slowly diffuses into the large reservoir of unreacted taurinate in the bulk. While this mechanism holds up to pressures of ~2.5 bar, at higher pressures, the CO_2-carrying species is carbamic acid.

The high storage capacity of ~0.58 mol CO_2 per mol IL in the near-surface region, already at CO_2 pressures as low as 0.9 mbar, that is, very similar to the atmospheric CO_2 partial pressure of 0.3 mbar, might trigger new process concepts for CO_2 absorption with this type of ionic liquids: one could envisage to absorb CO_2 in a spray tower where small droplets with a high surface-to-volume ratio are generated. Moreover, the preparation of high surface area materials, that is, in the form of supported thin films, could open attractive ways to capture CO_2 from air or exhaust gases in a more efficient manner.

4. EXPERIMENTAL SECTION

Near-ambient pressure XPS (NAP-XPS, also denoted as ambient pressure XPS or high pressure XPS) was performed with a home-built UHV system (base pressure 1×10^{-9} mbar) that allows gas dosage of a maximum background pressure of 1 mbar. It comprises a modified X-ray source (Specs XR 50) and a modified electron analyzer (Omicron EA 125 U7) (for details of the setup, see ref 25). XP spectra were measured at a pass energy of 50 eV using nonmonochromatized Al Kα radiation ($h\nu$ = 1486.6 eV) at a power of 50 W (U = 13 kV), resulting in an overall resolution of ~1.1 eV. The inelastic mean free path λ for photoelectrons in organic compounds at the kinetic energies used (~0.8−1.3 keV) is about 2.3−3.0 nm.[22] For measurements at normal emission (0°), the resulting XPS probing depth, also called information depth, ID (= 3λ), from which 95% of the signal originates, amounts to 7−9 nm. Thus, the XPS measurements average over several layers of the near-surface region. It is important to note that the 0.9 mbar CO_2 gas phase during the NAP XPS measurements does not change ID within the IL (it only decreases the overall IL signal intensity), as long as the IL signals are still detectable and as long as no overlap between gas phase and IL signals occurs, which is the case in our experiments.

The spectra of the CO_2 purged sample (Supporting Information) were measured with a modified VG Escalab 200 system using non-monochromatized Mg Kα radiation ($h\nu$ = 1253.6 eV, Specs XR 50 X-ray source) at a power of 50 W (U = 12.5 kV) and a VG Scienta R3000 electron analyzer. A pass energy of 100 eV was used, resulting in an overall resolution of ~0.8 eV.

The XP spectra were analyzed using the CasaXPS software (version 2.3.16Dev6). A two point linear background subtraction was applied. All peaks were fitted using a Gaussian−Lorentzian profile with 30% Lorentz contribution.

For both systems, IL films of ~0.1 mm thickness were prepared by deposition onto a planar Au foil. These samples were then introduced into the UHV chambers via a load lock with a time delay of approximately 5 min. The in situ heating of the IL was carried out by resistance heating. The sample temperature was measured with an absolute error of ±5 K, using a type K thermocouple attached to the Au foil.

The NAP-XP spectra were scaled to account for the signal intensity loss resulting from damping by the gas phase and a necessary change of sample position during measurement. The scaling factors for the gas phase damping correction were calculated by

dx.doi.org/10.1021/ja410745a | J. Am. Chem. Soc. 2014, 136, 436−441

$$\ln \frac{I}{I_0} = -\frac{\sigma_e d_{eff} p}{kT}$$

where I is the damped signal intensity, I_0 is the signal intensity in UHV without gas dosage, σ_e is the electron scattering cross section, and d_{eff} is the effective path length through the gas phase.[25] σ_e depends on the electron kinetic energy; σ_e values from a systematic study on electron scattering in CO_2 by Garcia and Manero[30] were used to derive a calibration curve for the kinetic energy region 500−3000 eV, from which the respective cross sections for the O 1s, N 1s, C 1s, and S 2p core level electrons at a kinetic energy of approximately 945, 1085, 1200, and 1318 eV were determined. A reference measurement with our NAP-XPS setup for the Pt 4p, 4d, and 4f core levels of an inert Pt sample confirmed the correctness of our calibration factors with an error of ±2.5%. The necessary change in sample position during the XPS measurements was corrected for by the normalization to overall N 1s intensity, which must remain constant during CO_2 application; thereby the reasonable assumption was made that ion density within the near-surface region remains unchanged during CO_2 application.

CO_2 (99.995% purity) was dosed onto the sample from the background while recording XP spectra. Contributions of minor traces of water to the observed O 1s signal are ruled out; this was done by measuring XP spectra while codosing 0.4 mbar water to 0.5 mbar CO_2, which left the O 1s signal and also the other XP signals unchanged. Furthermore, it is interesting to note that no increase in O 1s intensity was observed in CO_2 exposure experiments with nonamine functionalized ILs.

The isothermal absorption experiments under equilibrium conditions using bulk ionic liquid samples were carried out in an isothermal gas absorption apparatus consisting of a storage vessel (257 mL) and an absorption vessel (113 mL). The absorption vessel was filled with a known amount of ionic liquid and was completely evacuated (10^{-3} mbar). This pressure was maintained in the apparatus for 16 h to ensure the absence of any leak in the absorption vessel.

For the measurement, the storage vessel was pressurized with CO_2. The absorption at 310 K constant temperature was started with opening the valve connecting the storage and the absorption vessel. During the absorption experiment, the absorption medium was stirred with a magnetic stirrer at 250 rpm. Due to the small amount of absorption medium (0.250−0.500 g), the stirrer was not completely covered by the medium, which formed a compact viscous film at the bottom of the vessel. Simultaneously, the pressure was recorded using a Greisinger MSD 6 BAE pressure transducer. When the pressure in the absorption vessel remained constant for more than 16 h, the system was considered to be at equilibrium. The amount of absorbed CO_2 was calculated from the difference between the added CO_2 in the storage vessel and the resulting equilibrium pressure assuming the ideal gas law. The IR-spectra were recorded using a Jasco FT/IR-4100 spectrometer. The IR spectra of the CO_2-pressurized IL samples were transferred to the spectrometer and measured directly after the absorption experiment.

■ ASSOCIATED CONTENT

Ⓢ Supporting Information

Figures S1−S4 as described in the text. This material is available free of charge via the Internet at http://pubs.acs.org.

■ AUTHOR INFORMATION

Corresponding Authors

florian.maier@fau.de
christian.papp@fau.de

Notes

The authors declare no competing financial interest.

■ ACKNOWLEDGMENTS

The authors gratefully acknowledge the funding of the German Research Council (DFG) through grant Ste 620/9-1 and by the Cluster of Excellence "Engineering of Advanced Materials" (www.eam.uni-erlangen.de) at the Universität Erlangen-Nürnberg.

■ REFERENCES

(1) Ramdin, M.; de Loos, T. W.; Vlugt, T. J. H. *Ind. Eng. Chem. Res.* **2012**, *51*, 8149.
(2) Rochelle, G. T. *Science* **2009**, *325*, 1652.
(3) Huang, J. H.; Ruther, T. *Aust. J. Chem.* **2009**, *62*, 298.
(4) Brennecke, J. E.; Gurkan, B. E. *J. Phys. Chem. Lett.* **2010**, *1*, 3459.
(5) Soutullo, M. D.; Odom, C. I.; Wicker, B. F.; Henderson, C. N.; Stenson, A. C.; Davis, J. H. *Chem. Mater.* **2007**, *19*, 3581.
(6) Karadas, F.; Atilhan, M.; Aparicio, S. *Energy Fuels* **2010**, *24*, 5817.
(7) Hasib-ur-Rahman, M.; Siaj, M.; Larachi, F. *Chem. Eng. Process.* **2010**, *49*, 313.
(8) Xie, H. B.; Johnson, J. K.; Perry, R. J.; Genovese, S.; Wood, B. R. *J. Phys. Chem. A* **2011**, *115*, 342.
(9) Blanchard, L. A.; Hancu, D.; Beckman, E. J.; Brennecke, J. F. *Nature* **1999**, *399*, 28.
(10) Wasserscheid, P., Welton, T., Eds. *Ionic Liquids in Synthesis*, 2nd ed.; Wiley-VCH: Weinheim, 2008.
(11) Bates, E. D.; Mayton, R. D.; Ntai, I.; Davis, J. H. *J. Am. Chem. Soc.* **2002**, *124*, 926.
(12) Gálan Sánchez, L. M.; Meindersma, G. W.; de Haan, A. B. *Chem. Eng. J.* **2011**, *166*, 1104.
(13) Goodrich, B. F.; de la Fuente, J. C.; Gurkan, B. E.; Zadigian, D. J.; Price, E. A.; Huang, Y.; Brennecke, J. F. *Ind. Eng. Chem. Res.* **2011**, *50*, 111.
(14) Gurkan, B. E.; de la Fuente, J. C.; Mindrup, E. M.; Ficke, L. E.; Goodrich, B. F.; Price, E. A.; Schneider, W. F.; Brennecke, J. F. *J. Am. Chem. Soc.* **2010**, *132*, 2116.
(15) Wu, C.; Senftle, T. P.; Schneider, W. F. *Phys. Chem. Chem. Phys.* **2012**, *14*, 13163.
(16) Lui, M. Y.; Crowhurst, L.; Hallett, J. P.; Hunt, P. A.; Niedermeyer, H.; Welton, T. *Chem. Sci.* **2011**, *2*, 1491.
(17) Li, X. Y.; Hou, M. Q.; Zhang, Z. F.; Han, B. X.; Yang, G. Y.; Wang, X. L.; Zou, L. Z. *Green Chem.* **2008**, *10*, 879.
(18) Knöfel, C.; Martin, C.; Hornebecq, V.; Llewellyn, P. L. *J. Phys. Chem. C* **2009**, *113*, 21726.
(19) Danon, D.; Stair, P. C.; Weitz, E. *J. Phys. Chem. C* **2011**, *115*, 11540.
(20) Bacsik, Z.; Ahlsten, N.; Ziadi, A.; Zhao, G. Y.; Garcia-Bennett, A. E.; Martin-Matute, B.; Hedin, N. *Langmuir* **2011**, *27*, 11118.
(21) Masuda, K.; Ito, Y.; Horiguchi, M.; Fujita, H. *Tetrahedron* **2005**, *61*, 213.
(22) Roberts, R. F.; Allara, D. L.; Pryde, C. A.; Buchanan, D. N. E.; Hobbins, N. D. *Surf. Interface Anal.* **1980**, *2*, 5.
(23) Lovelock, K. R. J.; Deyko, A.; Licence, P.; Jones, R. G. *Phys. Chem. Chem. Phys.* **2010**, *12*, 8893.
(24) Steinrück, H.-P. *Phys. Chem. Chem. Phys.* **2012**, *14*, 5010.
(25) Pantförder, J.; Pöllmann, S.; Zhu, J. F.; Borgmann, D.; Denecke, R.; Steinrück, H.-P. *Rev. Sci. Instrum.* **2005**, *76*, 014102.
(26) Haynes, W. M.; Lide, D. R. *CRC handbook of chemistry and physics: a ready-reference book of chemical and physical data*, 93rd ed.; CRC Press: Boca Raton, FL, 2012.
(27) Lewis, T.; Faubel, M.; Winter, B.; Hemminger, J. C. *Angew. Chem., Int. Ed.* **2011**, *50*, 10178.
(28) Bossa, J.-B.; Borget, F.; Duvernay, F.; Theulé, P.; Chiavassa, T. *J. Phys. Chem. A* **2008**, *112*, 5113.
(29) Lovelock, K. R. J.; Kolbeck, C.; Cremer, T.; Paape, N.; Schulz, P. S.; Wasserscheid, P.; Maier, F.; Steinrück, H.-P. *J. Phys. Chem. B* **2009**, *113*, 2854.
(30) Garcia, G.; Manero, E. *Phys. Rev. A* **1996**, *53*, 250.